

**Showcasing research from Professor Guangming Huang's laboratory, School of Chemistry and Materials Science, University of Science and Technology of China, Hefei, P. R. China.**

**Introducing charge tag *via* click reaction in living cells for single cell mass spectrometry**

*In situ* derivatization for single cell mass spectrometry was accomplished via a biocompatible click reaction in single living cells. Permanently charged quaternary ammonium, as charge tag, was coupled with cysteine to further improve the ionization efficiency of induced nanoelectrospray mass spectrometry measurements. Therefore, this new protocol offers an opportunity to achieve the *in situ* quantifying cysteine levels and monitoring of its dynamic alterations in single living cells. Our study provides a general amplification strategy to expand the range of detectable metabolites for single cell mass spectrometry.

**As featured in:**



See Guangming Huang *et al.*,  
*Chem. Sci.*, 2020, 11, 7308.

Cite this: *Chem. Sci.*, 2020, **11**, 7308

All publication charges for this article have been paid for by the Royal Society of Chemistry

Introducing charge tag *via* click reaction in living cells for single cell mass spectrometry†Meihui Zhuang,<sup>‡a</sup> Zhuanghao Hou,<sup>‡a</sup> Peiyao Chen,<sup>a</sup> Gaolin Liang<sup>ID a</sup> and Guangming Huang<sup>ID \*ab</sup>

For single living cell mass spectrometry measurement, sensitivity is of great significance due to the extremely complicated chemical components of the cytoplasm. Higher sensitivity is always highly desired, especially for chemicals with low concentrations or poor mass spectrometry responses. Here, a quaternary ammonium salt group-based charge tag was designed to enhance the analytical performance for cysteine within single cells using induced nanoelectrospray mass spectrometry. While the charge tag was coupled to the analyte *via* biocompatible click reaction, viability of the living cells was maintained during *in situ* derivatization and following analysis. Enhanced sensitivity under physiological conditions for cysteine, at pH 7.4 and with highly concentrated salts, was achieved due to higher ionization efficiency of the charge tag. Therefore, the cysteine levels in single living HeLa cells and HepG2 cells were found to be in the range of  $62.0 \pm 3.4 \mu\text{M}$  and  $49.6 \pm 7.2 \mu\text{M}$ , respectively. Furthermore, the low cysteine levels in living single HeLa cells could be monitored, in the presence of cystine transporter inhibitor. Thus, this method provides a general strategy for *in situ* chemical derivatization for signal amplification in the field of single cell mass spectrometry.

Received 15th January 2020

Accepted 23rd June 2020

DOI: 10.1039/d0sc00259c

rsc.li/chemical-science

## Introduction

Single cell mass spectrometry (SCMS) metabolic studies provide the opportunity to further the current understanding of biological variability and differential response to disease and therapeutics.<sup>1–3</sup> Various metabolites in single blastomeres (with a spherical diameter of approximately 250  $\mu\text{m}$  and a cell volume of approximately 90 nL) from a 16-cell embryo have been revealed by SCMS.<sup>4</sup> However, metabolic studies in regular mammalian single cells remain challenging due to low picoliter (pL) volume, variation in metabolite types and levels, and lack of amplification technologies.<sup>5</sup>

In recent years, great efforts have been spent in this field to develop various SCMS techniques, including matrix-assisted laser desorption ionization MS,<sup>6</sup> direct sampling electrospray ionization (ESI),<sup>7–11</sup> patch-capillary electrophoresis-MS,<sup>12</sup> and patch clamp-ESI-MS.<sup>13</sup> However, many metabolites are still undetectable possibly due to their low concentration, or poor MS response. Recently, ambient MS combined with an immunoassay platform was developed by Bai<sup>14,15</sup> and Badu-Tawiah<sup>16</sup>

for the detection of proteins and glycans on cell surfaces, with the introduction of charge tags to greatly improve sensitivity, and the limit of detection was confirmed at cell numbers of as low as 25.<sup>14</sup> Thus, it is reasonable to assume that a greater understanding of metabolism would be obtained if a similar protocol could be extended for metabolite measurement at the single living cell level.

To achieve that goal, we intended to introduce a similar charge tag that requires the protocol to be simple, efficient, and cell biocompatible. Thus, a biocompatible click reaction was adopted. Ever since the original discovery from a firefly body between 2-cyanobenzothiazole (CBT) and cysteine (Cys),<sup>17,18</sup> CBT has been widely utilized in fluorescence (fluorophore-conjugated),<sup>18,19</sup> magnetic resonance (gadolinium-containing),<sup>20,21</sup> and positron emission tomography (<sup>18</sup>F-labeling)<sup>22</sup> probes for biomolecular analysis.

Herein, the quaternary ammonium group was covalently bonded with CBT to form the charge tag we designed as [(2-cyano-benzothiazol-6-ylcarbonyl)-methyl]-trimethylammonium (NCBT), for the purpose of MS signal amplification and increased MS sensitivity for Cys detection. We also introduced induced nanoelectrospray ionization (InESI),<sup>23</sup> as modified nESI, to provide a stable MS signal for pL-level samples and to overcome severe ion suppression effects from concentrated salt and derivatization reagent solutions.<sup>24,25</sup> The use of a charge tag, click reaction, and the InESI MS technique allowed the sensitivity and efficiency of Cys detection to be increased for analysis of single living cells and serum.

<sup>a</sup>Hefei National Laboratory for Physical Sciences at the Microscale, School of Chemistry and Materials Science, University of Science and Technology of China, Hefei, Anhui, 230026, P. R. China. E-mail: gmhuang@ustc.edu.cn

<sup>b</sup>National Synchrotron Radiation Laboratory, University of Science and Technology of China, Hefei, Anhui, 230029, P. R. China

† Electronic supplementary information (ESI) available. See DOI: 10.1039/d0sc00259c

‡ These authors contributed equally to this work contributed equally to this work.



## Results and discussion

### Workflow for single cell mass spectrometry of Cys in single living cells

In detail, Cys was coupled to NCBT *via* click reaction for adding a charge tag (permanently charged quaternary ammonium group) to enhance the MS response. The workflows for cell treatment (Fig. S1†) and subsequent SCMS measurement are illustrated in Fig. 1. Briefly, the cells were incubated in culture medium containing NCBT and then rinsed with phosphate-buffered saline (PBS) solution. Then, the cytoplasm of the incubated cells was withdrawn using borosilicate glass pipettes by applying approximately 75 kPa negative pressure for 1 min. The glass pipette was pulled to 1–2  $\mu\text{m}$  i.d., and then, the pipette was filled with pipette solution and controlled with a micro-manipulator. Next, the pipette was removed from the cell and subjected to InESI-MS (Detailed information could be found in experimental sections). Compared to Cys without a charge tag, the MS signal intensity of NCBT–Cys could be increased up to 75-fold in aqueous solution due to the fact that permanently charged ions dominate the charge competition during the ionization process. Furthermore, Cys in single living HeLa cells and HepG2 cells was successfully detected due to the *in situ* derivatization within living cells. The detailed structure of NCBT is illustrated in Scheme S1 and characterized in Fig. S2.†

### Highly efficient and biocompatible click reaction in living cells

To maximize the NCBT–Cys click reaction in living cells under physiological conditions, this click condensation reaction was tested at different pH values, NCBT concentrations, and reaction times. Fortunately, the highest reaction efficiency for the NCBT–Cys click reaction was found at a pH of 7.4 (Fig. 2a), which was significantly higher than that in acid solutions (pH of 5 and 6). The reaction efficiency at higher pH could not be

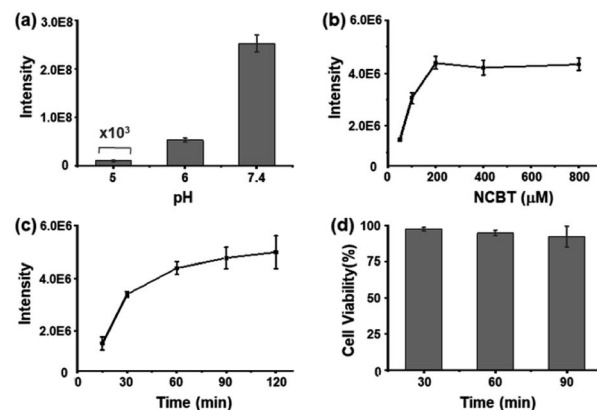


Fig. 2 Highly efficient and biocompatible click reaction in living cells. (a) Effect of solution pH values on NCBT–Cys click reaction. Reaction conditions: 10  $\mu\text{M}$  Cys and 200  $\mu\text{M}$  NCBT in pure  $\text{H}_2\text{O}$  solution at 37  $^\circ\text{C}$  for 1 h; formic acid was used to regulate the solution pH values. (b) NCBT concentration optimization experiment. HepG2 cells (approximately  $1 \times 10^5$ ) were incubated with different concentrations of NCBT (50–800  $\mu\text{M}$ ) in serum-free culture medium at 37  $^\circ\text{C}$  for 1 h, and then, the cells were washed with PBS solution and lysed in 100  $\mu\text{L}$  pure  $\text{H}_2\text{O}$  solution. (c) NCBT incubation time optimization experiment. HepG2 cells (approximately  $1 \times 10^5$ ) were incubated with 200  $\mu\text{M}$  NCBT in serum-free culture medium at 37  $^\circ\text{C}$  for different times (15–120 min), and then, the cells were washed with PBS solution and lysed in 100  $\mu\text{L}$  pure  $\text{H}_2\text{O}$  solution. (d) MTT assay of the effect of NCBT on HepG2 cells. The MTT proliferation assay estimated the cell viability (%) of HepG2 cells cultured in the presence of 200  $\mu\text{M}$  NCBT at 37  $^\circ\text{C}$  for 30, 60, and 90 min. All error bars denote s.d.;  $n = 3$ .

determined due to the hydrolysis of NCBT.<sup>22</sup> The above results were well in accordance with the CBT-based click-reaction, which was originally found in living fireflies.<sup>17,18</sup>

To obtain the maximum signal intensity of NCBT–Cys in living cells, the incubation concentration and time of NCBT were optimized using HepG2 as model cells. HepG2 cells were incubated with NCBT at concentrations of 50–800  $\mu\text{M}$  and time of 15–200 min, and then lysed for analysis. The incubation concentration and time of NCBT were set as 200  $\mu\text{M}$  (Fig. 2b) and 1 h (Fig. 2c), respectively. The cell viability was studied *via* MTT assay, which indicated, 98%, 95%, or 92% of HepG2 cells survived after being incubated with 200  $\mu\text{M}$  NCBT for 30, 60, or 90 min, respectively (Fig. 2d), suggesting that there is satisfactory biological compatibility between NCBT and single living cells for experiments. In addition, NCBT had little effect on the metabolites of single living HeLa cells (Fig. S3†).

### Improved Cys detection performance *via* click reaction

To evaluate the enhanced performance of Cys detection with NCBT derivatization, 10  $\mu\text{M}$  Cys with and without NCBT (200  $\mu\text{M}$ ) in aqueous solution were tested. For 10  $\mu\text{M}$  Cys, much lower ion intensity was obtained (as  $[\text{Cys} + \text{H}]^+$ ,  $m/z$  122.0287, intensity approximately  $3.2 \times 10^6$ ), while the intensity with NCBT derivatization was found to be approximately 75-fold higher (as  $[\text{NCBT-Cys}]^+$ ,  $m/z$  379.0881, intensity approximately  $2.4 \times 10^8$ ), as shown in Fig. 3a. To further evaluate the

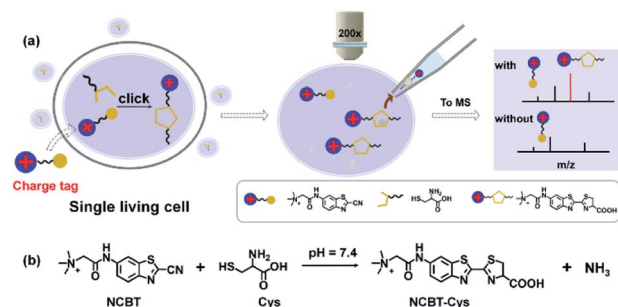


Fig. 1 Schematic of workflow for SCMS of Cys in single living HeLa and HepG2 cells. (a) Three steps were included: (i) *in situ* derivatization to couple the quaternary ammonium group (charge tag) with Cys under physiological condition to maintain cell viability (in serum-free medium, with humid atmosphere of 5%  $\text{CO}_2$  at 37  $^\circ\text{C}$ , pH 7.4), (ii) single living cell sampling *via* micropipette controlled with micromanipulator, and (iii) MS measurement of NCBT–Cys ( $m/z$  379.0881) with improved MS response over protonated Cys ( $m/z$  122.0278) due to enhanced ionization efficiency. (b) Biocompatible click reaction between NCBT and Cys; HeLa and HepG2 cells were incubated with NCBT (200  $\mu\text{M}$ ) for 1 h without significant cell death.





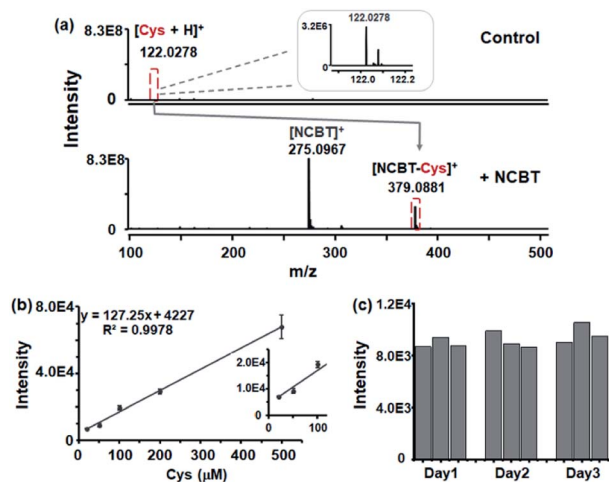


Fig. 3 Enhanced performance of Cys detection via click reaction. (a) MS spectra of 10  $\mu\text{M}$  Cys without (control, top) and with (+NCBT, down) 200  $\mu\text{M}$  NCBT in pure  $\text{H}_2\text{O}$  solution for 1 h. The scale of the signal intensity for both MS spectra was set as  $8.3 \times 10^8$ . Inset indicates the magnified (260 fold) Cys MS spectra signal. (b) Calibration curve of NCBT-Cys in artificial intracellular solution. Various amounts of Cys (ranging from 20 to 500  $\mu\text{M}$ ) were reacted with 200  $\mu\text{M}$  NCBT for 1 h. (Inset demonstrates the lower level (20–100  $\mu\text{M}$ ) of the calibration curve). (c) Nine repeated measurements of 50  $\mu\text{M}$  Cys in artificial intracellular solution were made over three consecutive days. Artificial intracellular fluid was composed of the following components: potassium chloride 140 mM, sodium chloride 6 mM, magnesium chloride 29 mM, ammonium bicarbonate 10 mM, glucose 10 mM, and HEPES 10 mM (pH was adjusted to 7.4). All error bars denote s.d.;  $n = 3$ .

sensitivity for the proposed method, the linear dynamic curve in artificial intracellular solutions was obtained for Cys in the presence of NCBT ( $[\text{NCBT-Cys}]^+$ ,  $m/z$  379.0881). As shown in Fig. 3b, the linear dynamic was observed from 20 to 500  $\mu\text{M}$ , which was sufficient to cover the Cys level in living cells (30–200  $\mu\text{M}$ ).<sup>26</sup> However, without the derivatization step, even 100  $\mu\text{M}$

Cys could not be detected in artificial intracellular solution (shown in Fig. S4†).

Next, the reproducibility of the present method was evaluated through nine repeated measurements over three consecutive days, with three measurements per day. The interday relative standard deviations (RSDs) were calculated to be 4.3%, 7.8%, and 8.1% with three continuous days, and intraday RSDs were calculated to be 4.3% (Fig. 3c). Thus, NCBT derivatization via click reaction significantly improved the MS signal response for Cys in the presence of highly concentrated salts. In addition, the click reaction-based derivatization was found to significantly increase the sensitivity for total Cys in serum, and other chemicals could also be detected in the presence of NCBT (shown in Fig. S5 and Table S1†).

### In situ monitoring of the Cys level and its dynamic alterations in single living cells

Finally, the proposed method was used for *in situ* monitoring of Cys levels in single living cells, which is of great significance for cell function, physiological regulation, and disease progression. Cys plays vital roles in cellular processes, cellular growth, protein synthesis, maintaining redox homeostasis, mitigating damage from free radicals and toxins, and the pathogenesis of a wide range of diseases.<sup>27,28</sup> HepG2 cells and HeLa cells were chosen as models, and the cells were incubated in serum-free DMEM medium with 200  $\mu\text{M}$  NCBT for 1 h. The corresponding full mass spectra are shown in Fig. 4a, with detailed spectra enlarged in Fig. 4b. It was found that, only for NCBT-incubated cells, NCBT-Cys ( $m/z$  379.0881) could be detected with typical ion intensity of approximately  $1.5 \times 10^4$  (84.7  $\mu\text{M}$ ), while raw Cys in cells with or without NCBT incubation remained undetectable. As shown in Fig. 4c, the Cys levels in single HeLa and HepG2 cells were also evaluated as  $62.0 \pm 3.4 \mu\text{M}$  and  $49.6 \pm 7.2 \mu\text{M}$ , respectively, based on the above-mentioned linear dynamic curve in Fig. 3b. The above intracellular Cys levels were consistent with previous reports that ranged from 30 to 200  $\mu\text{M}$ .<sup>26</sup> A variety of other metabolite molecules in single living cells could also be detected, and they were listed in Table S2.† Thus, the current method successfully allowed detection of Cys in single living cells.

The present method also enables the monitoring of dynamic alterations of cellular Cys levels under stimulation by the cystine transporter inhibitor erastin. Erastin acts on the cystine/glutamate antiporter to inhibit cystine uptake, which is vital to the formation of Cys, and thus, erastin stimulation would lead to a significant downregulation of the Cys level.<sup>29</sup> HeLa cells were treated with 0.5, 1.5, or 5  $\mu\text{M}$  erastin for 2 h before being subjected to NCBT derivatization and MS measurement. As shown in Fig. 4d, cells treated with 1.5  $\mu\text{M}$  or 5.0  $\mu\text{M}$  erastin exhibited significantly decreased levels of Cys, which is well in accordance with the results from a previous study.<sup>29</sup> The above single cell results were also verified with cell lysates (Fig. S6†).

## Conclusion

In summary, a simple, sensitive, and biocompatible SCMS method based on introducing a charge tag via click reaction and

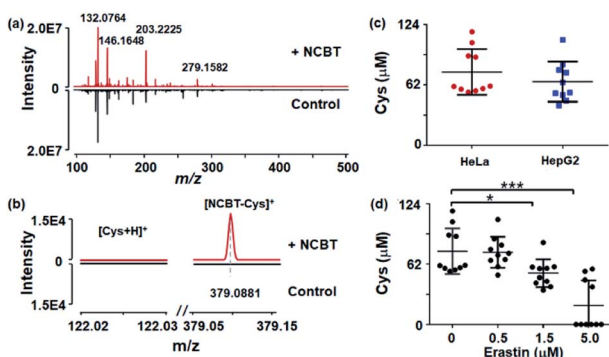


Fig. 4 *In situ* monitoring of the Cys level and its dynamic alterations in single living cells. (a) MS spectra obtained from single living HeLa cells with (+NCBT) and without (control) NCBT derivatization. (b) The expanded view of MS spectra of protonated Cys ( $m/z$  122.0278) and NCBT-Cys ( $m/z$  379.0881). (c) MS signal intensity of NCBT-Cys in HeLa cells (red dots,  $n = 10$ ) and HepG2 cells (blue squares,  $n = 10$ ). (d) The MS signal intensity of  $m/z$  379.0881 (NCBT-Cys) in HeLa cells after erastin stimulation at different concentrations ( $P < 0.05$  correlated by false discovery rate). \* denotes  $P < 0.05$ ; \*\*\* denotes  $P < 0.001$ .



InESI-MS was provided to greatly enhance the MS response of the chemicals in single cells. To our knowledge, this is the first report describing a charge tag combined with the CBT-Cys click reaction to be used for *in situ* derivatization of chemicals with low MS response in SCMS. We were able to monitor the intercellular level of specific cellular metabolites (e.g., Cys) in single living cells.

Although the detection of Cys was demonstrated as a proof-of-principle, this strategy for signal amplification *via* introducing charge tags can easily and readily be extended to other metabolites, with proper derivatization reagents. The overall throughput for the present method is approximately 5 min per cell, which might be greatly improved *via* combination with flow cytometry, when the sensitivity of NCBT derivatization is further enhanced.

Our study provides a general protocol to expand the range of detectable metabolites without the need to further improve the MS instrument. With all the efforts (more sensitive MS instruments and novel methodology development) to push forward SCMS metabolite detection, much wider applications can be anticipated for clinical diagnosis, understanding disease pathogenesis, and therapeutic drug discovery.

## Experimental section

### Materials and reagents

Cysteine (Cys), formic acid, and erastin were obtained from Sigma-Aldrich Chemical Co., Ltd. (St. Louis, MO, U.S.A.). 2-Cyano-6-aminobenzothiazole (CBT) was obtained from Shanghai Chemical Pharm-Intermediate Tech. Co., Ltd. (Shanghai, China). Tris-(2-carboxyethyl)-phosphine hydrochloride (TCEP), fetal bovine serum (FBS), glucose, 2-[4-(2-hydroxyethyl)-1-piperazinyl]ethanesulfonic acid (HEPES), 3-(4,5-dimethylthiazol-2-yl)-2,5-diphenyltetrazolium bromide (MTT), and Dulbecco's modified Eagle's medium (DMEM) were purchased from Sangon Biotech Co., Ltd. (Shanghai, China). Trifluoroacetic acid (TFA), sodium chloride, potassium chloride, and sodium hydroxide were supplied by Sinopharm Chemical Reagent Co., Ltd. (Shanghai, China). Betaine hydrochloride, isobutyl chloroformate, acetonitrile (high-performance liquid chromatography grade) were purchased from J&K Scientific Ltd. (Beijing, China), and 4-methylmorpholine was obtained from Aladdin Chemistry Co., Ltd. (Shanghai, China). All reagents were used without any further purification. Ultrapure water (18.2 MΩ cm) was obtained from a Milli-Q System (Millipore Corp., U.S.A.).

### Cell culture

The hepatocellular carcinoma HepG2 or human cervical carcinoma HeLa cells were cultured in DMEM supplemented with 10% FBS, penicillin (100 U mL<sup>-1</sup>), and streptomycin (100 μg mL<sup>-1</sup>). The cells were expanded in cell culture dishes and maintained in a humid atmosphere of 5% CO<sub>2</sub> at 37 °C. The medium was changed every other day.

### Treatment with erastin

HeLa cells were incubated with different concentrations (0.5, 1.5, and 5 μM) of erastin in culture medium for 2 h and then

maintained in a humid atmosphere of 5% CO<sub>2</sub> at 37 °C. Then, the cells were incubated with 200 μM NCBT in serum-free medium for 1 h and maintained in a humid atmosphere of 5% CO<sub>2</sub> at 37 °C. The other experimental steps were the same as those for the single cell sampling procedure.

### Serum sample preparation

To reduce the disulfide bonds of Cys, 10 μL of freshly prepared 300 g L<sup>-1</sup> TCEP solution was added to 90 μL FBS and incubated at 37 °C for 15 min. Then, 2.2 μL 10 mM NCBT was added for derivatization of analytes for 60 min. To precipitate protein, 200 μL 0.1% formic acid and 0.05% TFA in acetonitrile were added, and the FBS mixture was centrifuged for 2 min at 10 000×g (Minimax17, KeCheng, China). The clear supernatant was analyzed by InESI MS.

### MTT assay

Cytotoxicity was measured using the 3-(4,5-dimethylthiazol-2-yl)-2,5-diphenyltetrazolium bromide (MTT) assay with HepG2 cells. Cells growing in log phase were seeded at approximately 5 × 10<sup>3</sup>/well into 96-well cell culture plates. The cells were incubated at 37 °C under 5% CO<sub>2</sub> for 12 h. A solution of 200 μM NCBT (150 μL per well) in serum-free medium was added to the wells. The cells were incubated for 30, 60, or 90 min at 37 °C under 5% CO<sub>2</sub>. A solution of 5 mg mL<sup>-1</sup> MTT dissolved in phosphate-buffered saline (PBS, pH 7.4) was added to each well (15 μL per well) of the 96-well plate. After 4 h of incubation, the medium in the wells was carefully removed, and dimethyl sulfoxide (150 μL per well) was added to each well to dissolve the formazan. The data were obtained using an enzyme-linked immunosorbent assay (ELISA) reader (Varioskan Flash, Thermo Scientific) to detect the solution absorption at 490 nm. The formula used to calculate the viability of cell growth is as follows: cell viability (%) = (average of absorbance value of treatment group/average of absorbance value of control group) × 100.

### Single cell sampling procedure

The cells were incubated with or without 200 μM NCBT in serum-free culture medium for 1 h and maintained in a humid atmosphere of 5% CO<sub>2</sub> at 37 °C. Then, the cells were washed with PBS (pH 7.4) three times and finally stored in PBS solution. Single-cell micropipette sampling was performed with a Burleigh micromanipulator and Olympus CK2 inverted microscope. A sampling micropipette containing 185 mM NH<sub>4</sub>HCO<sub>3</sub> and 80 mM NH<sub>4</sub>Cl was attached to the micromanipulator and then inserted into single cells. The intracellular chemical constituents were obtained from the assayed cells by applying approximately 75 kPa negative pressure through a syringe connected to the glass pipettes for 1 min. Then, the pipette was removed and analysed *via* the InESI-MS device as previously described.<sup>13,23</sup>

### Instruments for InESI and MS

After extraction of the cytoplasmic chemical constituents from cells, the capillary micropipette was coupled to the InESI device.



An AC voltage with an amplitude of 3 kV at approximately 500 Hz was applied to the outside of the spray capillary micropipette. The tip of the micropipette was placed approximately 5 mm away from the orifice of the MS instrument. The MS experiments were performed using an orbitrap mass spectrometer (Exactive Plus, Thermo Fisher Scientific, San Jose, CA, U.S.A.), and tandem mass spectrometry (MS/MS) was conducted with an LTQ mass spectrometer (Thermo Scientific, San Jose, CA, U.S.A.). The MS instrument conditions throughout the experiments were as follows: S lens radio frequency level, 50% (positive mode); capillary temperature, 275 °C; mass resolution, 70 000; microscan, 1; and maximum ion injection time, 10 milliseconds. InESI-MS analysis for all samples were performed in positive mode. The data were acquired *via* Xcalibur software. The sampling micropipettes were pulled from borosilicate glass capillaries (1.2 mm o.d., 0.9 mm i.d.) by using a P-2000 laser-based micropipette puller (Sutter Instruments, Novato, CA, U.S.A.) with the size of 1–2  $\mu\text{m}$  (i.d.).

## Conflicts of interest

There are no conflicts to declare.

## Acknowledgements

We acknowledge support from the National Key Research and Development Program of China (2016YFA0201302 and 2019YFA0405603), the National Natural Science Foundation of China (21775143 and 21475121), the Innovative Program of Development Foundation of Hefei Center for Physical Science and Technology (2017FXCX003), the Users with Excellence Project of Hefei Science Center CAS (2018HSC-UE001, 2018HSC-UE016), and the Fundamental Research Funds for the Central Universities.

## Notes and references

- 1 S. J. Altschuler and L. F. Wu, *Cell*, 2010, **141**, 559–563.
- 2 S. S. Rubakhin, E. V. Romanova, P. Nemes and J. V. Sweedler, *Nat. Methods*, 2011, **8**, S20–S29.
- 3 R. Zenobi, *Science*, 2013, **342**, 1201.
- 4 R. M. Onjiko, S. A. Moody and P. Nemes, *Proc. Natl. Acad. Sci. U. S. A.*, 2015, **112**, 6545–6550.
- 5 A. Schmid, H. Kortmann, P. S. Dittrich and L. M. Blank, *Curr. Opin. Biotechnol.*, 2010, **21**, 12–20.
- 6 A. Amantonico, P. L. Urban, S. R. Fagerer, R. M. Balabin and R. Zenobi, *Anal. Chem.*, 2010, **82**, 7394–7400.
- 7 M. L. Tejedor, H. Mizuno, N. Tsuyama, T. Harada and T. Masujima, *Anal. Chem.*, 2012, **84**, 5221–5228.
- 8 T. Fujii, S. Matsuda, M. L. Tejedor, T. Esaki, I. Sakane, H. Mizuno, N. Tsuyama and T. Masujima, *Nat. Protoc.*, 2015, **10**, 1445–1456.
- 9 L. W. Zhang, D. P. Foreman, P. A. Grant, B. Shrestha, S. A. Moody, F. Villiers, J. M. Kwake and A. Vertes, *Analyst*, 2014, **139**, 5079–5085.
- 10 L. Zhang and A. Vertes, *Anal. Chem.*, 2015, **87**, 10397–10405.
- 11 L. W. Zhang, N. Khattar, I. Kemenes, G. Kemenes, Z. Zrinyi, Z. Pirger and A. Vertes, *Sci. Rep.*, 2018, **8**, 1227.
- 12 J. T. Aerts, K. R. Louis, S. R. Crandall, G. Govindaiah, C. L. Cox and J. V. Sweedler, *Anal. Chem.*, 2014, **86**, 3203–3208.
- 13 H. Zhu, G. Zou, N. Wang, M. Zhuang, W. Xiong and G. Huang, *Proc. Natl. Acad. Sci. U. S. A.*, 2017, **114**, 2586–2591.
- 14 S. Xu, W. Ma, Y. Bai and H. Liu, *J. Am. Chem. Soc.*, 2019, **141**, 72–75.
- 15 W. Ma, S. Xu, H. Nie, B. Hu, Y. Bai and H. Liu, *Chem. Sci.*, 2019, **10**, 2320–2325.
- 16 S. Chen, Q. Wan and A. K. Badu-Tawiah, *J. Am. Chem. Soc.*, 2016, **138**, 6356–6359.
- 17 E. H. White, F. McCapra and G. F. Field, *J. Am. Chem. Soc.*, 1963, **85**, 337–343.
- 18 H. Ren, F. Xiao, K. Zhan, Y.-P. Kim, H. Xie, Z. Xia and J. Rao, *Angew. Chem., Int. Ed.*, 2009, **48**, 9658–9662.
- 19 Y. Yuan, J. Zhang, Q. Cao, L. An and G. Liang, *Anal. Chem.*, 2015, **87**, 6180–6185.
- 20 G. Liang, J. Ronald, Y. Chen, D. Ye, P. Pandit, M. L. Ma, B. Rutt and J. Rao, *Angew. Chem., Int. Ed.*, 2011, **50**, 6283–6286.
- 21 Z. J. Hai, Y. H. Ni, D. Saimi, H. Y. Yang, H. Y. Tong, K. Zhong and G. L. Liang, *Nano Lett.*, 2019, **19**, 2428–2433.
- 22 J. Jeon, B. Shen, L. Xiong, Z. Miao, K. H. Lee, J. Rao and F. T. Chin, *Bioconjugate Chem.*, 2012, **23**, 1902–1908.
- 23 G. Huang, G. Li and R. G. Cooks, *Angew. Chem., Int. Ed.*, 2011, **50**, 9907–9910.
- 24 G. Y. Li, S. M. Yuan, Y. Pan, Y. Z. Liu and G. M. Huang, *Anal. Chem.*, 2016, **88**, 10860–10866.
- 25 Y. T. Chen, G. Y. Li, S. M. Yuan, Y. Pan, Y. Z. Liu and G. M. Huang, *Anal. Chem.*, 2019, **91**, 10441–10447.
- 26 J. Liu, Y.-Q. Sun, Y. Huo, H. Zhang, L. Wang, P. Zhang, D. Song, Y. Shi and W. Guo, *J. Am. Chem. Soc.*, 2014, **136**, 574–577.
- 27 K. G. Reddie and K. S. Carroll, *Curr. Opin. Chem. Biol.*, 2008, **12**, 746–754.
- 28 C. E. Paulsen and K. S. Carroll, *Chem. Rev.*, 2013, **113**, 4633–4679.
- 29 S. J. Dixon, K. M. Lemberg, M. R. Lamprecht, R. Skouta, E. M. Zaitsev, C. E. Gleason, D. N. Patel, A. J. Bauer, A. M. Cantley, W. S. Yang, B. Morrison III and B. R. Stockwell, *Cell*, 2012, **149**, 1060–1072.

